A Recurring Pattern of Chromosomal Aberrations in Mammary Gland Tumors of MMTV-*cmyc* Transgenic Mice

Zoë A. Weaver,[1]* Stephen J. McCormack,[2] Marek Liyanage,[1] Stan du Manoir,[1] Allen Coleman,[3] Evelin Schröck,[1] Robert B. Dickson,[2] and Thomas Ried[1]

[1]Genome Technology Branch, National Human Genome Research Institute, NIH, Bethesda, Maryland
[2]The Lombardi Cancer Center, Georgetown University Medical Center, Washington, D.C.
[3]Laboratory of Genetics, National Cancer Institute, NIH, Bethesda, Maryland

Mice carrying the MMTV-*cmyc* transgene develop mammary tumors at 9 to 12 months of age. Little is known about karyotypic changes in this model of human breast cancer. We have developed and applied molecular cytogenetic techniques to study chromosomal aberrations that occur in these tumors, namely, comparative genomic hybridization and spectral karyotyping. Cell lines from eight tumors were established and analyzed, four of which carried a heterozygous *p53* mutation. All of the tumor cell lines revealed increases in ploidy and/or multiple numerical and structural chromosomal aberrations. No consistent differences were observed between *cmyc*/*p53*$^{+/+}$ and *cmyc*/*p53*$^{+/-}$ tumors, suggesting that *cmyc* induces karyotype instability independent of *p53* status. Loss of whole chromosome (Chr) 4 was detected in five of the eight tumors. Parts of Chr 4 are syntenic to human 1p31–p36, a region that is also deleted in human breast carcinomas. Four tumors carried translocations involving the distal portion of Chr 11 (syntenic to human chromosome arm 17q), including two translocations T(X;11), with cytogenetically identical breakpoints. We compare the pattern of chromosomal aberrations with human breast cancers, find similarities in several syntenic regions, and discuss the potential of an interspecies cytogenetic map of chromosomal gains and losses. *Genes Chromosomes Cancer 25:251–260, 1999.*

INTRODUCTION

Karyotyping serves as a first comprehensive survey of genetic alterations in human cancers. The abundance of cytogenetic information in hematologic malignancies and solid tumors has produced both diagnostically and prognostically relevant information and has contributed to the positional cloning of cancer causing genes (Heim and Mitelman, 1995). However, efforts to understand the sequence of genetic aberrations during carcinogenesis and attempts to establish test systems for novel therapeutics depend increasingly on murine models of human cancers. The analysis of chromosome aberrations in mouse models of carcinogenesis has relied mainly on chromosome banding techniques. All mouse chromosomes are acrocentric and of similar size, which makes their identification difficult. Consequently, data on recurring chromosome aberrations in mouse models are rare.

In order to explore the cytogenetic profile of a mouse model for human breast cancer, we have applied molecular cytogenetic screening techniques, namely, comparative genomic hybridization (CGH) and spectral karyotyping (SKY), to evaluate eight cell lines that were established from primary mammary gland tumors in mice that overexpress the *cmyc* oncogene under the control of the MMTV-LTR promoter. CGH detects DNA copy number changes in human and murine tumor genomes after hybridization of differentially labeled tumor and normal DNA (Kallioniemi et al., 1992; du Manoir et al., 1995; Shi et al., 1997). SKY allows the visualization of all tumor chromosomes in different colors by combining spectral imaging with fluorescence in situ hybridization (FISH) using combinatorially labeled mouse chromosome painting probes. SKY greatly facilitates karyotyping of the small acrocentric mouse chromosomes and is particularly useful for the analysis of highly rearranged tumor chromosomes (Liyanage et al., 1996; Coleman et al., 1997).

Mouse models for human breast cancer have become valuable tools for the study of tumorigen-

Zoë Weaver's and Thomas Ried's present address is Genetics Department, Division of Clinical Sciences, National Cancer Institute, NIH, Bethesda, MD.

Stephen J. McCormack's present address is Institute for Biosciences, Bioinformatics and Biotechnology, George Mason University, Manassas, VA.

Marek Liyanage's present address is Aurora Biosciences Corporation, San Diego, CA.

Stan du Manoir's present address is Institut de Génétique et de Biologie Moléculaire et Cellulaire, Ilkirch Cu de Strasbourg, France.

*Correspondence to: Dr. Zoë Weaver, Genetics Department, Division of Clinical Sciences, National Cancer Institute, 49 Convent Drive, Bethesda, MD 20892. E-mail: weaverz@mail.nih.gov

Received 18 September 1998; Accepted 21 January 1999

esis. The MMTV-*cmyc* transgenic mouse strain was the earliest transgenic breast cancer model described (Stewart et al., 1984). It was developed to examine the consequences of *cmyc* overexpression in mouse mammary tissue, based on the observation that amplification of the *MYC* gene is common in human breast cancer (reviewed in Nass and Dickson (1997)). The long (7–14 months) latency period prior to the development of mammary tumors in MMTV-*cmyc* mice and the requirement for multiple pregnancies suggested that additional events besides *cmyc* overexpression were required for cellular transformation (Stewart et al., 1984; Leder et al., 1986), such as mutations in the tumor suppressor protein p53. The *TP53* gene is frequently deleted or mutated in human tumors, and in *Wnt-1* transgenic mice its absence accelerates mammary tumorigenesis [Donehower et al., 1995]. The role of *p53* in tumorigenesis in MMTV-*cmyc* transgenic mice was examined by mating to a $p53^{-/-}$ strain [Elson et al., 1995; McCormack et al., 1998]. The results suggested that formation of mammary tumors was not accelerated by the absence of a single *p53* allele. In the $p53^{-/-}$ mice, lymphomas arose so rapidly that it was not possible to evaluate the relevance of *p53* mutation with respect to mammary gland tumorigenesis. However, lack of p53 protein clearly influenced mammary gland development, and the glands exhibited hyperplastic lobular growth [McCormack et al., 1998].

Because both *cmyc* overexpression and *p53* mutation are associated with genomic instability in transformed cells [Livingstone et al., 1992; Taylor et al., 1997], we wanted to examine the consequences of *cmyc* overexpression and lack of a single *p53* allele in mouse mammary tumors. In a previous study, we performed preliminary SKY analysis of early-passage cultured cells from a few MMTV-*cmyc* mammary tumors [McCormack et al., 1998]. Here, we extended that study for a comprehensive evaluation of karyotypic abnormalities using SKY. Furthermore, we performed whole-genome analysis on all tumor cell lines using CGH. The combination of SKY and CGH data results in a more detailed understanding of the cytogenetic events involved in mammary tumorigenesis in the MMTV-*cmyc* mouse model than was hitherto possible. By comparing the pattern of chromosomal aberrations in mouse and human mammary carcinomas, we evaluated the potential of comparative cytogenetics and the establishment of syntenic maps for understanding the relevance of these aberrations.

MATERIALS AND METHODS

Tumor Cell Lines and Culture

Mammary epithelial cell lines were derived from mammary tumors (average latency approximately 190 days) of MMTV-*cmyc*/$p53^{+/+}$ and MMTV-*cmyc*/$p53^{+/-}$ mice. FVB (MMTV-*cmyc*) and 129/Sv-*Trp53* mice were mated to produce those genotypes, but only littermates of the varying genotypes were compared to neutralize any background effects of the two strains. Tumor bearing animals were sacrificed and cell lines prepared from the tumor tissue as described previously [Amundadottir et al., 1995; McCormack et al., 1998].

DNA for CGH and metaphase chromosomes for SKY were prepared from the cell lines at early-passage numbers (passages 6–9). Normal control DNA was prepared from tail or spleen tissue of mice of the same genotype. Normal metaphase chromosomes for CGH were prepared from the spleens of C57BL/6 mice. The spleens were crushed in a homogenizer and cultured for 48 hr in RPMI + 20% fetal bovine serum with the addition of 6 μg/ml concanavalin A (Sigma, St. Louis, MO), 25 μg/ml lipopolysaccaride (Boehringer Mannheim, Indianapolis, IN), and 60 μl of 0.5% β-mercaptoethanol per 50 ml of medium. After an additional 5 hr incubation in 30 μg/ml of bromodeoxyuridine (Sigma) and 0.15 μg/ml of fluorodeoxyuridine (Sigma), 0.1 μg/ml Colcemid (Gibco BRL, Grand Island, NY) was added for 15 min. The cells were lysed in hypotonic solution (0.075 M KCl) and the chromosomes were fixed in methanol:acetic acid (3:1). Metaphase chromosomes for SKY were obtained from the same tumor cells in culture (passages 5–8) by incubation of the cells in 0.1 μg/ml Colcemid for 5 hr, followed by cell lysis in 0.06 M KCl and subsequent fixation in methanol:acetic acid (3:1).

Comparative Genomic Hybridization

DNA labeling, hybridization, and detection were performed by standard procedures. Control reference DNA and tumor cell DNA were labeled with digoxigenin-12-dUTP and biotin-16-dUTP (Boehringer Mannheim), respectively, by nick translation. Five hundred ng of each labeled DNA was precipitated together with an excess (40 μg) of the Cot-1 fraction of mouse genomic DNA (Gibco BRL). This probe DNA mixture was resuspended in 10 μl of hybridization solution (50% formamide, 2 × SSC, 10% dextran sulfate), denatured for 5 min at 80°C, and preannealed at 37°C for 1–2 hr. Normal metaphase chromosomes from spleen cultures of C57BL/6 mice were dropped onto glass slides and

pretreated with 0.1 mg/ml RNAse A (Boehringer Mannheim), followed by 10 μg/ml pepsin (Sigma) in 0.01 M HCl. The chromosomes were denatured in 70% formamide, 2× SSC at 75°C for 1.5 min prior to application of the probe DNA mixture. Hybridization was carried out under a coverslip at 37°C for 2–4 days, after which the biotinylated tumor DNA was detected with FITC conjugated to avidin (Vector Laboratories), and the digoxigenin-labeled normal DNA was detected with a mouse antidigoxin antibody, followed by a TRITC-conjugated anti-mouse antibody (Sigma). The slides were counterstained with DAPI for chromosome identification.

CGH Image Acquisition and Analysis

Gray-level images were acquired using a cooled charge-coupled device (CCD) camera (CH250, Photometrics, Tucson, AZ) mounted on a Leica DMRBE epifluorescence microscope. Sequential exposures through filters specific to each fluorochrome (TR1, TR2, TR3; Chroma Technology, Brattleboro, VT) were recorded. Quantitation of CGH results was performed using a custom computer program developed for the analysis of mouse chromosomes (based on a human CGH program as described in du Manoir et al. [1995]). In a modification of the human CGH program, threshold levels for the final ratio profile were established empirically using mouse cell lines with known chromosomal gains and losses. The thresholds were defined as the value that would be expected in a diploid tumor cell population for a trisomy or monosomy of a certain chromosome in 50% of the test cells (i.e., 1.25 for a trisomy and 0.75 for a monosomy).

Spectral Karyotyping

Spectral karyotyping of the mammary tumor cell lines was performed as described previously [Liyanage et al., 1996; Schröck et al., 1996]. Spectral analysis of chromosomes was carried out using an epifluorescence microscope (Leica DMRBE) that was equipped with a SD200 SpectraCube (Applied Spectral Imaging, Migdal Ha'Emek, Israel) and a custom-designed filter cube (Chroma Technology, Brattleboro, VT) that allows for the simultaneous excitation of all dyes and the measurement of their emission spectra. To visualize the raw spectral image, different colors (blue, green, or red) were assigned to specific spectral ranges. Chromosomes then were unambiguously identified using a spectral classification algorithm that results in the assignment of a separate classification color to all pixels with identical spectra by use of SkyView software (Applied Spectral Imaging). Chromosome aberrations were defined using the nomenclature rules from the Committee on Standardized Genetic Nomenclature for Mice [Davisson, 1996]. For each tumor, 6–10 metaphases were analyzed.

RESULTS

CGH Reveals Recurrent Loss of Chromosome 4 and Gains of Chromosomes 11 and 8 in MMTV-*cmyc* Tumors

CGH is a screening test for chromosomal imbalances in tumor genomes. Here, we applied CGH to map chromosomal gains and losses in eight cell lines established from mammary gland tumors in MMTV-*cmyc* mice. Four of the tumors were wild-type for the *p53* tumor suppressor gene, and four were heterozygous for a *p53* mutation. The cell lines revealed numerous chromosomal gains and losses, structural aberrations, and changes in ploidy.

A summary of chromosomal copy number changes is presented in Figure 1. All chromosomes were involved in at least one gain or loss, but a nonrandom pattern emerged. The most consistent changes were partial or complete loss of Chr 4 in six of eight cases, gains of Chr 6 in three, partial gains of Chr 8 in three and of Chr 11 in three. The average number of copy alterations (ANCA) was 5.75 per tumor. The majority of chromosomal gains and losses involved entire chromosomes, rather than chromosomal regions (35 of 46 copy number changes). For example, five of the cell lines (three $p53^{+/-}$ and two $p53^{+/+}$) exhibited loss of entire Chr 4, whereas in 67a5 ($p53^{+/-}$), the copy number decrease was localized to band 4E. An increase in copy number of the entire Chr 11 occurred in two cases (myc 3; 67a5) and of 11D-E in another cell line (myc 83). We did not observe a higher number of copy alterations for the *p53* hemizygous mice than for the $p53^{+/+}$ mice. Previous analyses showed that all tumors from hemizygous mice retained one wild-type *p53* allele [McCormack et al., 1998].

Spectral Karyotyping Detects Structural Aberrations and Ploidy Changes

In order to describe the chromosomal mechanisms that result in recurring copy number changes in MMTV-*cmyc*–induced mammary gland carcinomas, we applied SKY to tumor metaphase chromosomes. In contrast to CGH, SKY also permits the visualization of balanced structural chromosomal aberrations. The pattern of chromosomal aberrations included numerical aberrations (whole-chromosome gains and losses), translocations, Robertsonian translocations, dicentric chromosomes, and

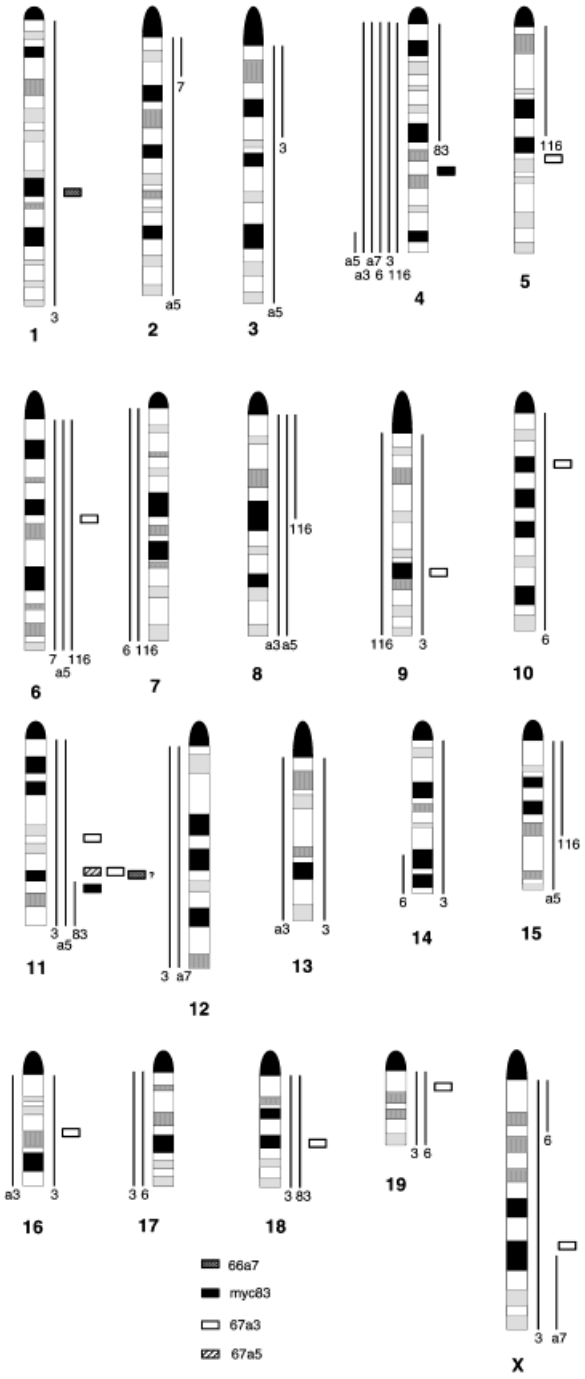

Figure 1. Karyogram of chromosomal aberrations in MMTV-*cmyc* tumor cells detected by CGH and SKY. Bars on the right side of the chromosome ideograms indicate gain and bars on the left side loss of genetic material. Individual tumor cell lines are indicated underneath the bars with the following abbreviations: 3 = myc3; 6 = myc6; 7 = myc7; 83 =myc83; a5 = 67a5; a7 =66a7; a3 =67a3; and 116 = 116br. Filled boxes indicate the breakpoints for the clonal aberrations listed in Table 1 (and the chromosomes in the Figure 2 insert), as determined by SKY analysis. The upper 67a3 box on Chr 11 indicates the T(5;11) breakpoint and the lower box indicates the T(X;11) breakpoint. The question mark symbol on Chr 11 refers to the T(Dp11;1) in 66a7 (Table 1), in which the region of duplication was approximated from the DAPI image.

deletions. Several of the tumor cell lines here were previously karyotyped (67a3, 67a5, 66a7, 116br, myc 83) [McCormack et al., 1998]. For this study, each cell line was passaged and rekaryotyped to ensure identical passage numbers for CGH and SKY analyses. Clonal aberrations listed in Table 1 take into account the total number of cells analyzed for each tumor. Some tumor cell lines (67a3, 67a5, myc 7) contained more than one subclone with shared marker chromosomes but variation in ploidy. Tumor 67a3 displayed a particularly complex karyotype, with five subclones that were derived from a clone containing only the unbalanced translocation T(5;11) (Fig. 2). Many of the cells also contained small deleted chromosomes. The detection of deletion breakpoints requires a band assignment that can be estimated by aligning the inverse DAPI-band image with the classification (Fig. 2, inset). Aberrations involving Chr 11 (in some cases more than one type) were observed in five of the cell lines by SKY analysis (Table 1). With the exception of the T(5;11) breakpoint in 67a3, which is in the same chromosome band (11B) as the mouse *trp53* gene, the breakpoints cluster in the distal region of Chr 11. 67a3 and myc 83 both contain a T(X;11) with cytogenetically identical breakpoints. A breakpoint map for all tumors is provided in Figure 1.

Higher-resolution analyses of chromosomal breakpoints can now be attempted using locus-specific FISH probes. For example, the Chr 11 breakpoint in the T(5;11) in 67a3 appears to be closer to the centromere than are breakpoints in myc 83, 67a5, or 66a7. Hybridization with a mouse *Brca1* cosmid probe determined that the portion of Chr 11 in the T(5;11) contains *Brca1*, and the position of the signal confirmed that the breakpoint is proximal to 11D (data not shown). All clonal aberrations observed by SKY are summarized in Table 1.

Correlation Between CGH and SKY

All cell lines were analyzed using both SKY and CGH, and the respective results were compared (Table 1). The data show that chromosomal gains and losses mapped by CGH could be confirmed at a single-cell level by SKY in most cases. In tumor myc 83, for example, a dicentric chromosome derived from Chr 4 was present. The CGH profile enabled us to determine precisely the region of Chr 4 that was present in this marker and demonstrated that bands A–D were duplicated (Fig. 3a,b). A copy number increase of Chr 18 mapped by CGH was identified as a trisomy 18 by SKY. The profile also facilitated the characterization of the translocation t(X;11) and defined the additional Chr 11 material as being derived from chromosome bands 11D–E.

Gain of Chr 11 was found in three cell lines by CGH, and SKY revealed an additional cluster of breakpoints in Chr 11B–E. An increase in copy

TABLE 1. Summary of Structural Aberrations Identified by SKY Analysis and Chromosomal Copy Number Changes Detected by CGH[a]

Cell line	Ploidy (SKY)[b]	CGH-detected[c] Losses	CGH-detected[c] Gains	SKY-detected[d] clonal structural aberrations, whole chromosome Losses	SKY-detected[d] clonal structural aberrations, whole chromosome Gains
myc Tg[e]					
myc 3	3n	**4**	1	**4**	
		12	3(A–D)	**12**	
				Del(8A)[f]	
		17	**9**	**17**	**9**
			11		**11**
			13		
			14		**14**
			16		
			18		**18**
			19		**19**
			X		
myc6	3n	**4**		**4**	7
		7	10		
		14(E)			11
		17			16
			19		**19**
			X(A1–4)		
myc7	2n and 4n		**2**(A)	**Del(2D–E)**	
			6		**6**
					15
myc83	2n		**4(A–C3)**	**Dic(4;4)(D;D)**[g]	
			11(D–E)	**T(XE;11D)**[h]	
			18		**18**
myc Tg[i] *p53+/−*					
67a3	3n	**4**		**4**	2
				9	3
		13	**8**	**13**	**8**
				Del(10B–D)	
		16		**16**	12
				19	15
				T(XE;11B5–C)	
				T(5E2;11B)	
				T(6C;19B)	
				T(18C;16B5–C1)	
67a5	3n	4(E)	**2**		**2**
			3		**3**
			6		**6**
			8		**8**
			11	**Del(11D–E)**	
			15		**15**
				+ many nonclonal structural aberrations	
66a7	2n	4	X(F)	T(Dp11C;1E2)[j]	
		12			
116br	4n–5n	**4**	5(A–D)	no structural aberrations, many inconsis-	
		7	6	tent gains or losses, including −4, −9	
		9	8(A–B)		
			15(A–D)		

[a]Karyotype nomenclature following the Committee on Standardized Genetic Nomenclature for Mice [Davisson, 1996].
[b]Ploidy of each clone was determined by SKY analysis.
[c]Copy number changes taken from the average ratio profile after CGH analysis of each cell line. Gains and losses that correspond to those recurrently identified in the SKY analysis are shown in bold.
[d]Aberrant chromosomes were identified by SKY analysis. Structural aberrations were considered clonal if present in two or more metaphases. Gains and losses were considered clonal if present in at least two or at least three metaphases, respectively. At least 10 metaphase cells were analyzed per tumor. SKY of primary cultures of tumors 67a3, 67a5, 66a7, 116br, and myc 83 was published previously [McCormack et al., 1998]. For this study additional cells were karyotyped and the clonal aberrations reflect the total number of cells analyzed.
[e]Mammary tumor cell lines made from MMTV-myc transgenic/$p53^{+/+}$ mice.
[f]Del: deleted chromosome that retains the centromere.
[g]Dic: dicentric chromosome.
[h]T: translocation. All observed translocations were nonreciprocal. By convention, the chromosome donating the centromere is listed first.
[i]Mammary tumor cell lines made from MMTV-myc transgenic/$p53^{+/-}$ mice.
[j]Dp: duplicated chromosome region.

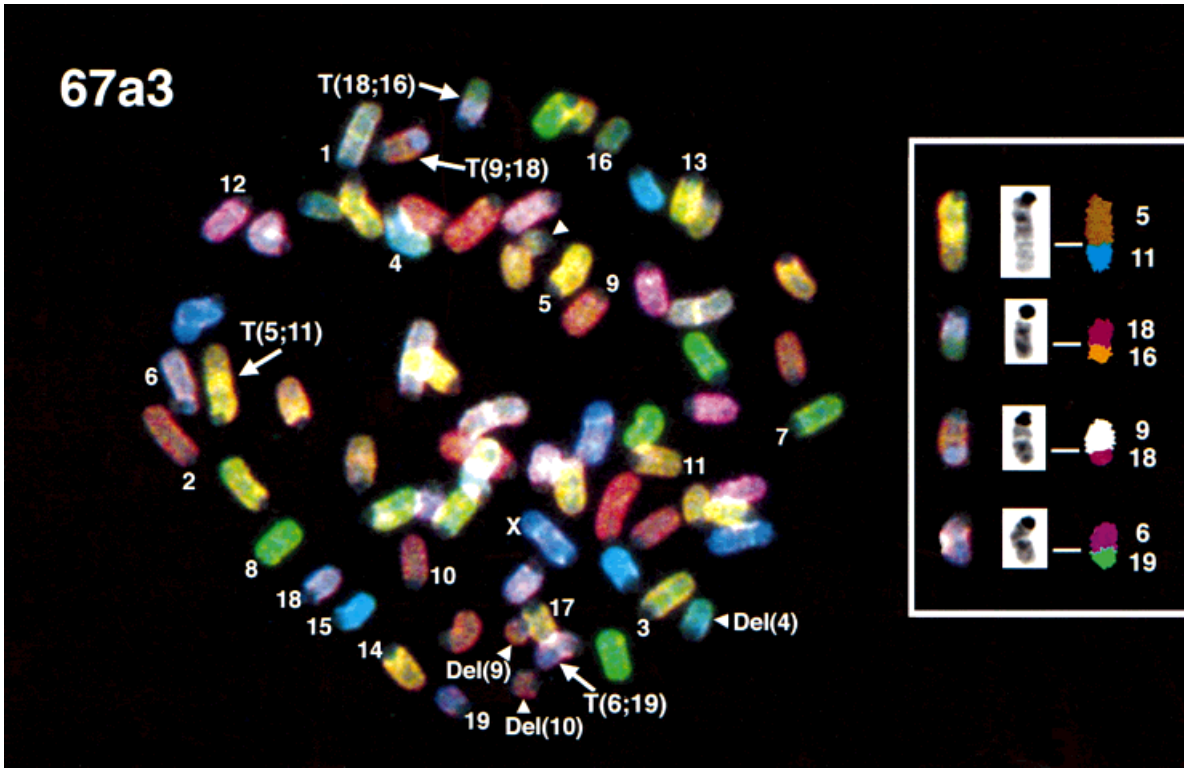

Figure 2. Spectral karyotyping analysis of a representative metaphase cell from mammary tumor cell line 67a3 (MMTV-*cmyc*/*p53*$^{+/-}$). One copy of each chromosome is numbered, and aberrant chromosomes are indicated by arrows. Arrowheads denote partially deleted chromosomes. The insert contains the translocation chromosomes visualized in display colors (left row), after DAPI-banding (inverted, center row), and after spectra-based classification in pseudocolors (right row). The karyotype of this tumor is 70,XX, +1, +2, −4, +8x2, +12, −13, −16, −19, +X, +Del(4D-E), +Del(9B-F), +Del(10B-D), +Del(11B-E), and the unbalanced translocations T(5E2;11B), T(6C;19B), T(9E;18D), and T(18C;16B5-C1).

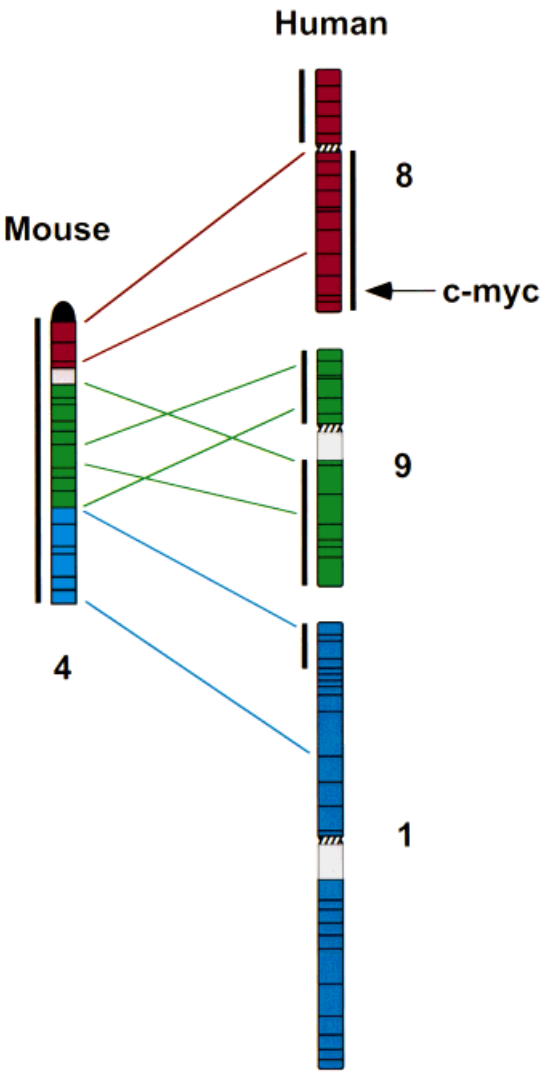

Figure 4. Schematic presentation of the syntenic portions of mouse Chr 4 and human chromosomes 8, 9, and 1. Regions syntenic to the human chromosomes are shown in red, green, or blue on mouse Chr 4, with corresponding colored bars to indicate approximately the involved bands. The bar on the left side of mouse Chr 4 represents the copy number losses seen in MMTV-*cmyc* mammary tumor cell lines, bars on the left and right of human chromosomes 8, 9, and 1 represent commonly found chromosomal gains (right) and losses (left) in primary human breast carcinomas [Nishizaki et al., 1997; Tirkkonen et al., 1998]. The map position of the human *MYC* gene on chromosome 8 is indicated by an arrow. Note that the syntenic region of human chromosome 8 that is part of the loss that involves mouse Chr 4, does not include the *MYC* gene. Information on syntenic regions was compiled from the Mouse Genome Informatics site on the World Wide Web (www.informatics.jax.org).

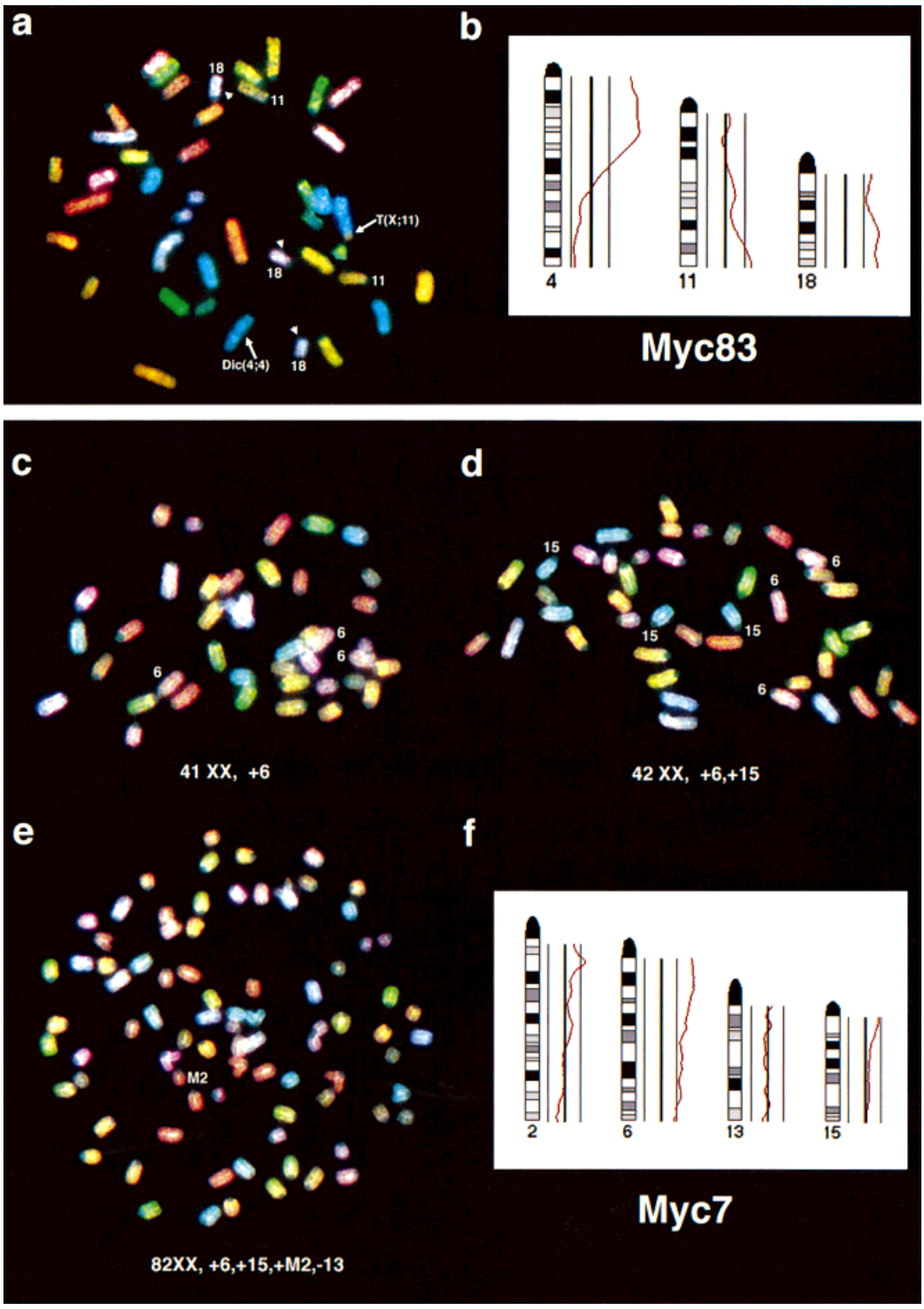

Figure 3. Comparison of CGH and SKY results for two tumor cell lines. **a:** SKY of a metaphase cell from the clonal myc 83 (MMTV-*cmyc*/*p53*$^{+/-}$) cell line, shown in display colors. Arrows indicate the aberrant chromosomes, and arrowheads denote three copies of Chr 18. The relevant ratio profiles from the CGH results are shown as red lines in **b**. The bold center line reflects a ratio of 1, and the two adjacent lines denote the threshold values for loss (left) or gain (right) of genetic material. The profiles confirm the gain of proximal Chr 4 due to the dicentric chromosome, identifying the part of Chr 11 in the T(X;11) as the 11D–E region, and reaffirming the gain of Chr 18. In contrast, SKY of myc 7 (MMTV-*cmyc*/p53$^{+/-}$) revealed three subclones (**c**–**e**) with an increase in ploidy involving Chrs 6 and 15, a marker chromosome derived from Chr 2 (M2), and tetraploidization in (e). The corresponding ratio profiles are shown in **f**; only the gain of Chr 6 is reflected, indicating the relative prevalence of clone (c).

number of the entire Chr 11 occurred in two cases (myc 3, 67a5) and of 11D–E in another cell line (myc 83).

Clonal heterogeneity cannot be identified by CGH. CGH detects chromosomal copy number changes only if they are present in at least 60% of the tumor cells. Figure 3 shows an example of the potential of SKY to identify clonal evolution and the mechanism of progressive chromosomal aberrations. By SKY analysis, myc 7 contains three subclones that most likely represent cytogenetic events that occur during tumor progression, because they contain an increasing number of aberrations. SKY images of the three clones are presented in the likely order of advancement: the gain of Chr 6 in a diploid metaphase cell (Fig. 3c), gains of Chrs 6 and 15 (Fig. 3d), and finally tetraploidization with additional gains and losses (Fig. 3e). Clone (Fig. 3c) is likely to be the predominant clone, because the gain of Chr 15 observed in clones (Fig. 3d) and (Fig. 3e) by SKY analysis is not reflected in the CGH profile. Therefore, the combined application of SKY and CGH not only facilitates the comprehensive characterization of the majority of chromosomal aberrations, but also provides relevant information with respect to the sequence in which these aberrations occur.

DISCUSSION

The molecular cytogenetic analyses of eight cell lines established from mammary gland adenocarcinomas in MMTV-*cmyc* transgenic mice has revealed a recurring pattern of chromosomal aberrations. Using CGH, 46 copy number alterations were mapped in eight cell lines, which results in an average number of copy alterations (ANCA) of 5.75. This number is comparable to the ANCA in human breast carcinomas [Ried et al., 1995]. Entire or partial loss of mouse Chr 4 was the most frequently observed cytogenetic abnormality in these tumors. In five carcinomas, the entire chromosome was lost, and in a sixth tumor (67a5), band 4E was deleted. A seventh tumor (myc 83) contains a partial gain of Chr 4, which includes all but bands 4D and 4E. Therefore the consensus region of chromosome loss maps to 4E. This region is syntenic to human 1p32–36 (Fig. 4) and is known to be a site of allelic loss in several cancers, suggesting that it harbors at least one tumor suppressor gene. Interestingly, in human breast cancer, allelic loss of 1p32–pter has been linked to *MYC* gene amplification and to a poor prognosis [Bièche et al., 1994; Tsukamoto et al., 1998].

Other regions of Chr 4 are syntenic to human chromosome arms 9p, 9q, 6q, and 8q (Fig. 4). Losses of chromosome arms 9p, 9q, and 6q have also been observed in primary human breast cancers and their metastases [Nishizaki et al., 1997; Tirkkonen et al., 1998]. Therefore, there is synteny of chromosomal gains and losses among mouse/human breast cancers that maps to human chromosomes 1p32–36, 6q, 9p, and 9q. In contrast, chromosome arm 8q is never lost in human breast carcinomas. Instead, this chromosome arm is frequently subject to copy number increases. Of note is that the distal region of human chromosome arm 8q that harbors the *MYC* oncogene is not part of the region of human chromosome arm 8q that is syntenic to mouse Chr 4. The endogenous mouse *cmyc* maps to Chr 15D, which is amplified in two MMTV-*cmyc* cell lines (67a5, 116br). One could therefore hypothesize that the whole-arm gain of 8q that is so commonly observed in human breast cancers has its main target in copy number increases for *MYC*. As an extension of this observation, the whole-arm 8q gain in human cancers may actually reflect the mechanism by which additional copies of *MYC* are acquired (such as isochromosome formation), and that copy number increases of genes that reside on human chromosome arm 8q bands syntenic to mouse Chr 4 are less important in mammary gland carcinogenesis.

We also noted the prevalence of Chr 11 rearrangements by SKY, and copy number increases mapped by CGH to a region that is syntenic to human chromosome bands 17q21–23. Chromosome arm 17q is frequently gained in human breast carcinomas. The mouse homologues of several genes involved in breast cancer were mapped to the distal region of Chr 11. For example, the *ERBB2* oncogene, mapping to human chromosome region 17q11–q21 and to mouse 11D, is commonly amplified in breast carcinomas [Bièche et al., 1996]. High-level amplifications of two different regions at 17q23 (also syntenic to mouse 11D) have been detected by CGH by several investigators [Kallioniemi et al., 1994; Ried et al., 1995; Bärlund et al., 1997].

The genetic changes we observed in the *cmyc* tumors may point to a tumor suppressor gene at the distal end of Chr 4, and a proto-oncogene on Chr 11, but a larger data set of mammary tumors is necessary before a strong connection can be made to each particular region. Very little research on genomic changes in mouse mammary tumors has been published. One study of mammary tumors in *Wnt-1* transgenic animals also found loss of whole Chr 4, but at a lower incidence than we found for *cmyc* tumors [Donehower et al., 1995]. It would be useful to perform comparative cytogenetic analyses

of mammary tumors induced by several different oncogenes overexpressed as transgenes (examplesof existing mouse models include *cerbB2*, *hras*, and *tgf*α transgenics).

It is clear that further screening of murine tumor genomes for recurring chromosome aberrations and genomic imbalances will be facilitated by the combined use of SKY and CGH. Analogous to other studies of human carcinomas [Ghadimi et al., 1999; Macville et al., 1999], SKY and CGH data for the mouse tumors are complementary, even though the comparison was difficult in those tumors that had multiple clones and ploidy variations. In agreement with data on human tumors of epithelial origin, the analysis of chromosome aberrations indicated that balanced structural aberrations were rare in this mouse model. Therefore, as in human breast cancers, the majority of aberrations result in genomic imbalances. In contrast, mouse models of hematologic malignancies display a pattern of balanced chromosomal aberrations that is also characteristic for human leukemias and lymphomas [Barlow et al., 1996; Coleman et al., 1997]. This observation of an apparently consistent mechanism of chromosomal aberrations adds to the validity of mouse models of human carcinogenesis. The establishment of a comprehensive comparative map of chromosomal gains, losses, and breakpoints for human and murine tumors could help us to assess the functional relevance of chromosomal copy number changes and translocations, and to define pivotal chromosomal regions for the development and progression of particular cancers. Comparative mapping will then help to validate current mouse models for human carcinogenesis, and it could further facilitate the identification of chromosomal loci whose involvement is critical in tumorigenesis beyond species boundaries.

ACKNOWLEDGMENTS

The authors thank Hesed Padilla-Nash, Merryn Macville, and Danny Wangsa for scientific advice and discussion, and Sandy Deming for technical assistance. Spectral karyotyping was developed under the terms of an NIH Cooperative Research and Development Agreement (CRADA #9512-8) with Applied Spectral Imaging, Inc.

REFERENCES

Amundadottir LT, Johnson MD, Merlino G, Smith G, Dickson RB. 1995. Synergistic interaction of transforming growth factor α and c-*myc* in mouse mammary and salivary gland tumorigenesis. Cell Growth Diff 6:737–748.

Barlow C, Hirotsune S, Paylor R, Liyanage M, Eckhaus M, Collins F, Shiloh Y, Crawley JN, Ried T, Tagle D, Wynshaw-Boris A. 1996. Atm deficient mice: a paradigm of ataxia-telangectasia. Cell 86:159–171.

Bärlund M, Tirkkonen M, Forozan F, Tanner MM, Kallioniemi O, Kallioniemi A. 1997. Increased copy number at 17q22–q24 by CGH in breast cancer is due to high-level amplification of two separate regions. Genes Chromosomes Cancer 20:372–376.

Bièche I, Champème M-H, Lidereau R. 1994. A tumor suppressor gene on chromosome 1p32-pter controls the amplification of *MYC* family genes in breast cancer. Cancer Res 54:4274–4276.

Bièche I, Tomasetto C, Regnier CH, Moog-Lutz C, Rio MC, Lidereau R. 1996. Two distinct amplified regions at 17q11–q21 involved in human primary breast cancer. Cancer Res 56:3886–3890.

Coleman AE, Schröck E, Weaver Z, du Manoir S, Yang F, Ferguson-Smith MA, Ried T, Janz S. 1997. Previously hidden chromosome aberrations in T(12;15)-positive BALB/c plasmacytomas uncovered by multicolor spectral karyotyping. Cancer Res 57:4585–4592.

Davisson MT. 1996. Rules for nomenclature of chromosome anamolies. In Lyon MF, Rastan S, Brown SDM, editors. Genetic variants and strains of the laboratory mouse, 3rd ed. New York: Oxford University Press, p 1443–1445.

Donehower LA, Godley LA, Aldaz CM, Pyle R, Shi YP, Pinkel D, Gray J, Bradley A, Medina D, Varmus HE. 1995. Deficiency of p53 accelerates mammary tumorigenesis in Wnt-1 transgenic mice and promotes chromosomal instability. Genes Dev 9:882–895.

du Manoir S, Schröck E, Bentz M, Speicher MR, Joos S, Ried T, Lichter P, Cremer T. 1995. Quantitative analysis of comparative genomic hybridization. Cytometry 19:24–41.

Elson A, Deng C, Campos-Torres J, Donehower LA, Leder P. 1995. The MMTV/c-*myc* transgene and p53 null alleles collaborate to induce T-cell lymphomas, but not mammary carcinomas in transgenic mice. Oncogene 11:181–190.

Ghadimi BM, Schröck E, Walker RL, Wangsa D, Jauho A, Meltzer PS, Ried T. 1999. Specific chromosomal aberrations and amplification of the AIB1 nuclear receptor coactivator gene in pancreatic carcinomas. Am J Pathol 154:525–536.

Heim S, Mitelman F. 1995. Cancer Cytogenetics, 2nd ed. New York: Wiley-Liss.

Kallioniemi A, Kallioniemi OP, Sudar D, Rutovitz D, Gray JW, Waldman F, Pinkel D. 1992. Comparative genomic hybridization for molecular cytogenetic analysis of solid tumors. Science 258:818–821.

Kallioniemi A, Kallioniemi OP, Piper J, Tanner M, Stokke T, Chen L, Smith HS, Pinkel D, Gray JW, Waldman FM. 1994. Detection and mapping of amplified DNA sequences in breast cancer by comparative genomic hybridization. Proc Natl Acad Sci USA 91:2156–2160.

Leder A, Pattengale PK, Kuo A, Stewart TA, Leder P. 1986. Consequences of widespread deregulation of the c-*myc* gene in transgenic mice: multiple neoplasms and normal development. Cell 45:485–495.

Livingstone LR, White A, Sprouse J, Livanos E, Jacks T, Tlsty TD. 1992. Altered cell cycle arrest and gene amplification potential accompany loss of wild-type p53. Cell 70:923–935.

Liyanage M, Coleman A, du Manoir S, Veldman T, McCormack S, Dickson RB, Barlow D, Wynshaw-Boris A, Janz S, Wienberg J, Ferguson-Smith MA, Schröck E, Ried T. 1996. Multicolour spectral karyotyping of mouse chromosomes. Nat Genet 14:312–315.

Macville M, Schröck E, Padilla-Nash H, Keck C, Ghadimi BM, Zimonjic D, Popescu N, Ried T. 1999. Comprehensive and definitive molecular cytogenetic characterization of HeLa cells by spectral karyotyping. Cancer Res 59:141–150.

McCormack SJ, Weaver Z, Deming S, Natarajan G, Torri J, Johnson MD, Liyanage M, Ried T, Dickson RB. 1998. *Myc*/p53 interactions in transgenic mouse mammary development, tumorigenesis and chromosomal instability. Oncogene 16:2755–2766.

Nass SJ, Dickson RB. 1997. Defining a role for c-*Myc* in breast tumorigenesis. Breast Cancer Res Treat 44:1–22.

Nishizaki T, DeVries S, Chew K, Goodson WH III, Ljung BM, Thor A, Waldman FM. 1997. Genetic alterations in primary breast cancers and their metastases: direct comparison using modified comparative genomic hybridization. Genes Chromosomes Cancer 19:267–272.

Ried T, Just KE, Holtgreve-Grez H, du Manoir S, Speicher MR, Schröck E, Latham C, Blegen H, Zetterberg A, Cremer T, Auer G. 1995. Comparative genomic hybridization of formalin fixed, paraffin embedded breast carcinomas reveals different patterns of chromosomal gains and losses in fibroadenomas and diploid and aneuploid carcinomas. Cancer Res 55:5415–5423.

Schröck E, du Manoir S, Veldman T, Schoell B, Wienberg J, Ferguson-Smith MA, Ning Y, Ledbetter DH, Bar-Am I, Soenksen D, Garini Y, Ried T. 1996. Multicolor spectral karyotyping of human chromosomes. Science 273:494–497.

Shi YP, Naik P, Dietrich WF, Gray JW, Hanahan D, Pinkel D. 1997. DNA copy number changes associated with characteristic LOH in islet cell carcinomas of transgenic mice. Genes Chromosomes Cancer 19:104–111.

Stewart TA, Pattengale PK, Leder P. 1984. Spontaneous mammary adenocarcinomas in transgenic mice that carry and express MTV/*myc* fusion genes. Cell 38:627–637.

Taylor C, Jalava A, Mai S. 1997. C-*Myc* dependent initiation of genomic instability during neoplastic transformation. Curr Topics Microbiol Immunol 224:201–207.

Tirkkonen M, Tanner M, Karhu R, Kallioniemi A, Isola J, Kallioniemi O. 1998. Molecular cytogenetics of primary breast cancer by CGH. Genes Chromosomes Cancer 21:177–184.

Tsukamoto K, Ito N, Yoshimoto M, Kasumi F, Akiyama F, Sakamoto G, Nakamura Y, Emi M. 1998. Allelic loss on chromosome 1p is associated with progression and lymph node metastasis of primary breast carcinoma. Cancer 82:317–322.